Mon. Not. R. Astron. Soc. **323**, 577–583 (2001)

Extensive serendipitous X-ray coverage of a flare star with *ROSAT*

J. D. Silverman,★ K. A. Eriksen, P. J. Green and S. H. Saar
Harvard-Smithsonian Center for Astrophysics, 60 Garden Street, Cambridge, MA 02138, USA

Accepted 2000 October 18. Received 2000 October 9; in original form 1999 November 17

ABSTRACT

We report the serendipitous discovery of a flare star observed with the *ROSAT* X-ray observatory. From optical spectra, which show strong and variable emission lines of the hydrogen Balmer series and neutral helium, we classify this object as a M3.0Ve star, and estimate a distance of 52 pc from published photometry. Owing to the close proximity of the star (13.6 arcmin) to the calibration source and RS CVn binary AR Lacertae, long-term X-ray coverage is available in the *ROSAT* archive (~50 h spanning 6.5 yr). Two large flare events occurred early in the mission (1990 June–July), and the end of a third flare was detected in 1996 June. One flare, observed with the Position Sensitive Proportional Counter (PSPC), had a peak luminosity $L_X = 1.1 \times 10^{30}$ erg s^{-1}, an e-folding rise time of 2.2 h and a decay time of 7 h. This decay time is one of the longest detected on a dMe star, providing evidence for the possibility of additional heating during the decay phase. A large High Resolution Imager (HRI) flare (peak $L_X = 2.9 \times 10^{30}$ erg s^{-1}) is also studied. The 'background' X-ray emission is also variable – evidence for low-level flaring or microflaring. We find that $\geqslant$59 per cent of the HRI counts and $\geqslant$68 per cent of the PSPC counts are caused by flares. At least 41 per cent of the HRI exposure time and 47 per cent of the PSPC are affected by detectable flare enhancement.

Key words: stars: flare – stars: late-type – X-rays: stars.

1 INTRODUCTION

X-ray emission from late-type M dwarfs has been studied extensively to investigate the structure and emission mechanisms of stellar coronae. Coronal heating to X-ray emitting temperatures is attributed to either impulsive flares or quiescent energy release in magnetic structures. The corona of these stars are thought to be similar to the Sun, but often with luminosities that are orders of magnitude higher. The high magnetic activity of these flare stars is also seen in their optical spectra. Continuum enhancement and strong emission lines of the H Balmer series, Ca II and neutral He are often evident (Montes et al. 1999).

An *EXOSAT* study (Pallavicini, Tagliaferri & Stella 1990) showed that flares have a wide range of energies and time-scales. Most outbursts can be described as either impulsive (decay time <1 h) or long-decay flares (decay time >1 h) and have thermal X-ray spectra with temperatures similar to solar X-ray flares. The impulsive stellar flares have time-scales similar to the compact solar flares. The long-duration flares have greater total energy and are more similar to two-ribbon flare events.

From *ROSAT* observations, coronal emission from dMe stars has been shown to have two distinct spectral components, a low-temperature component attributed to quiescent active regions and a variable, high-temperature component owing to compact flaring regions (Giampapa et al. 1996).

Schmitt (1994) has shown conclusively the existence of long-duration flares on M stars using the *ROSAT* all-sky survey. In some flaring stars, the long decay can be attributed to continual heating of the flaring region (Schmitt & Favata 1999; Ottmann & Schmitt 1996). New flare models have been developed (Reale & Micela 1998) in which the additional heating determines the characteristics of the decay. Using this model, an analysis of long-duration flares on AD Leo (Favata, Micela & Reale 2000b) and EV Lac (Favata et al. 2000a) have shown the emitting regions to be compact with length-scales of less than the stellar radius and similar in size to solar flares, thereby providing evidence that long-duration flares are produced in high-pressure structures.

During an analysis of observations with the *ROSAT* High Resolution Imager (HRI) of the RS CVn binary AR Lac, we noticed an X-ray source within the field of view to be highly variable and undetected in many fields. The first X-ray detection of this source was with the *Einstein* observatory (hence the catalogue name, 2E 2206.6+4517; Harris et al. 1993). Coaddition of six IPC observations spanning 26.6 ks yield a 4σ detection with 115 net counts. The source is undetected in a 1.5 ks HRI observation. No flaring activity is evident during these observations.

We analysed 39 observations from the *ROSAT* public data archive (16 PSPC; 23 HRI) which included this source position within the field of view. The total observing time was ≈50 h. The

★ E-mail: jds@head-cfa.harvard.edu

observations span two flares with almost complete light curves, the tail end of a third flare, and show variability in the low-level X-ray emission. The flare detected with the PSPC has a long decay time, possibly providing evidence for significant continual heating during the flare decay. Thus, a further in-depth study of flares and quiescent emission from 2E 2206.6+4517 could provide a useful test of current models.

2 OBSERVATIONS AND DATA REDUCTION

We detect the X-ray source 2E 2206.6+4517 in 16 observations with the *ROSAT* Position Sensitive Proportional Counter (PSPC) and 23 observations with the HRI, within the instrument bandpass of 0.1–2.4 keV. Extensive and continuous X-ray observations (≈17 h) were made with the PSPC between 1990 June 18–22 (during the *ROSAT* in-orbit calibration period), 1991 December 30–31, and 1993 May 29 and June 02. The HRI calibration observations of AR Lac began 13 d after the completion of the PSPC observations. 14 HRI pointings between 1990 July 2–8, include the source 2E 2206.6+4517. Eight additional HRI observations are available in the archive over the period of 1992 June through 1996 November for a total observing time of 33 h.

Table 1. *ROSAT* X-ray observations.

Seq. name	Obs. date	MJD	Exp. time (s)	Off-axis angle (arcmin)
rp100588	18/06/90–29/06/90	48060.13	27843.3	16.5
rp110586	19/06/90	48061.25	1945.2	29.3
rp110591	19/06/90	48061.53	1919.7	4.4
rp110599	19/06/90	48061.85	1986.5	19.2
rp110589	19/06/90–20/06/90	48061.85	1826.9	37.2
rp110592	20/06/90	48062.19	13932.7	28.3
rp110601	19/06/90–22/06/90	48061.98	3330.2	47.1
rp110590	20/06/90	48062.48	1885.0	10.5
rp110602	20/06/90	48062.79	2340.6	20.8
rp110595	20/06/90–21/06/90	48062.92	2132.7	27.4
rp110598	21/06/90–22/06/90	48063.85	2542.1	9.0
rp110596	20/06/90	48062.12	1838.5	39.3
rp110597	20/06/90	48062.05	2255.3	34.7
rp110600	19/06/90	48061.91	2011.2	45.5
rp160099^1	30/12/91–31/12/91	48620.26	13062.9	16.3
rp400278^1	29/05/93–02/06/93	49136.37	4702.8	16.3
rh100247	02/07/90	48074.14	20667.5	13.6
rh110249	02/07/90	48074.28	1419.7	17.7
rh110251	02/07/90	48074.48	1972.8	10.1
rh110252	02/07/90	48074.59	1687.1	13.5
rh110253	02/07/90	48074.66	2208.0	15.2
rh110254	02/07/90	48074.73	1933.6	8.7
rh110255	02/07/90	48074.80	1987.0	14.2
rh110259	03/07/90	48075.07	1700.6	16.2
rh110260	03/07/90	48075.14	1664.4	8.8
rh110261	03/07/90	48075.66	2264.7	4.0
rh110262	03/07/90	48075.86	2501.1	9.2
rh110267	04/07/90–05/07/90	48076.88	2124.4	17.8
rh110268	04/07/90	48076.94	1660.4	10.0
rh110269	05/07/90	48077.01	1619.7	1.6
rh110270	05/07/90	48077.07	1718.8	10.8
rh141876	10/06/92	48783.53	2437.5	13.6
rh202061	10/12/95	50061.04	5515.6	13.5
rh202062	11/12/95	50062.90	1919.7	13.5
rh202063	12/01/96–13/01/96	50094.89	19142.9	11.7
rh202159	03/06/96–04/06/96	50237.73	13664.0	13.5
rh202160	06/06/96	50240.05	4488.0	13.5
rh202161	09/07/96	50273.20	21157.0	13.6
rh180166	25/11/96–27/11/96	50413.38	3218.4	13.4

Notes: rp = PSPCC; rp^1 = PSPCB; rh = HRI.

We measured count rates using the IRAF/PROS data analysis software and corrected for vignetting caused by the large range of off-axis angles ($2 < \theta < 47$ arcmin). The observations were subdivided into multiple time bins to achieve a higher temporal resolution while preserving a minimal 2σ detection for each bin. An annular region was centred on the source to correct for the background count rate for most cases. For detections near the edge of the field, a nearby circular background region was chosen. A log of the *ROSAT* observations is given in Table 1 which includes the exposure time and off-axis angle.

Spectral fitting of the PSPC data was done with the XSPEC software package. Source and background counts were extracted using the XSELECT task from the FTOOLS package, and the ancillary response files were constructed with PCARF to account for off-axis vignetting. We ignored the lowest 11 spectral energy bins to avoid scattered solar extreme ultraviolet (EUV) contamination. The highest 56 spectral channels were also omitted because of poor statistics – a result of a marked decrease in the effective area of the instrument at these energies. The energy bin distribution oversamples the intrinsic spectral resolution of the PSPC, so we grouped the bins by a factor of 5 to improve the statistics.

Multiple optical spectra were taken by Perry Berlind with the Tillinghast 60 arcsec telescope and FAST spectrograph (Fabricant et al. 1998) at the Fred Lawrence Whipple Observatory on Mount Hopkins. A slit width of 3 arcsec, a 300 lines mm^{-1} grating, and the Loral charge-coupled device (CCD) with 15 μm pixels provided a resolution of ≈5 Å. A 3.5-min exposure was taken on UT 1998 May 16 and two 10-min exposures were acquired on UT 1998 May 30 and UT 1998 June 24. An observation of Feige 34 was used for extinction correction and flux calibration. Standard bias subtraction, flat-fielding, the extraction of one-dimensional spectra and wavelength calibration were performed using IRAF.

3 SOURCE IDENTIFICATION AND OPTICAL SPECTRA

After obtaining an X-ray source position from a nearly on-axis HRI observation, we identified two candidate optical counterparts within 10 arcsec on the Digitized Sky Survey red plates.

Two short observations were adequate to classify candidate 1 as an active Me star based on its Balmer emission, and candidate 2 as a normal G dwarf, with no evidence for a composite spectrum. We thus identify the Me star as the optical counterpart to 2E 2206.6+4517. Coordinates from the USNO-A2.0 catalogue (Monet et al. 1998) are $\alpha = 22^{h}08^{m}37\overset{s}{.}5$, $\delta = +45°31'27\overset{''}{.}9$ (J2000) and a 5-arcmin finder chart is provided in Fig. 1.

To facilitate an accurate spectral classification, the emission-line star was observed again on UT 1998 May 30 and UT 1998 June 24 for 10 min each. Both spectra showed strong emission lines, typical of a dMe flare star.

The first long spectrum (Fig. 2) showed strong emission lines, typical of a dMe flare star in an active flaring state. The second observation (Fig. 3) showed a marked decrease in the strength of the emission lines, indicating that the flare star was either in or close to quiescence. Table 2 lists the measured emission line equivalent widths (EQs). The strength of chromospheric heating owing to the flare is evident by the increase in the hydrogen line emission by a factor of 1.6 (Hα)–4.1 (Hγ).

The optical magnitudes from the USNO catalogue are $B = 16.5$ and $R = 14.2$ for this source, colours consistent with a late-type star. However, these colours may be affected by the strong

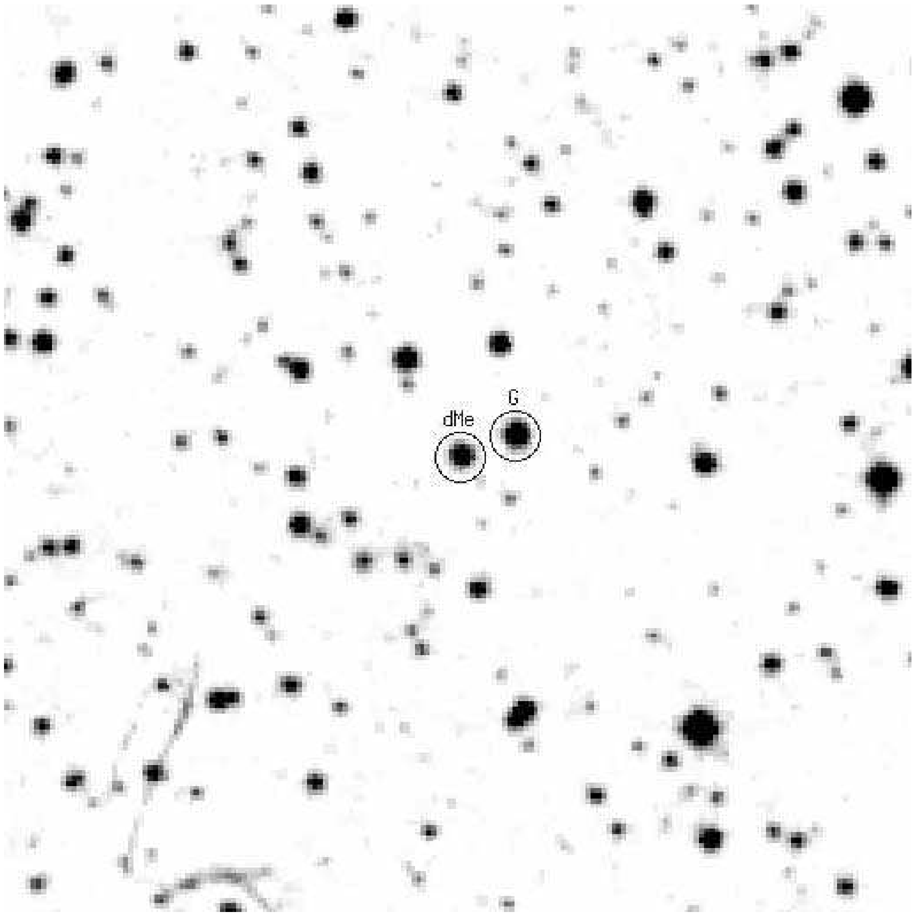

Figure 1. Digital Sky Survey plate showing the two possible optical counterparts to the X-ray flare. The star labelled dMe is the likely counterpart. The field of view is $5 \times 5\,\mathrm{arcmin}^2$ (north is up, east is left). The thin structures to the south-east are plate artefacts.

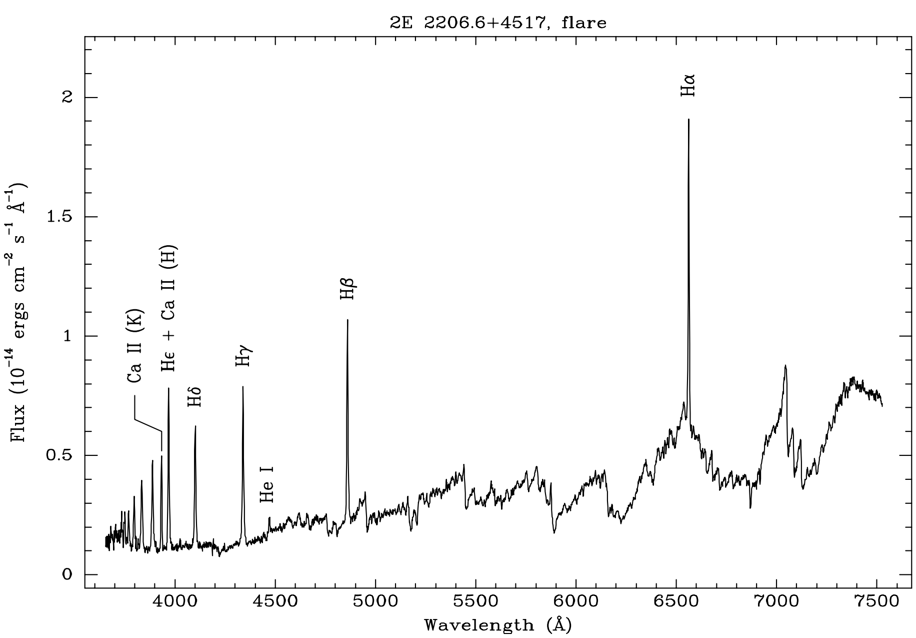

Figure 2. Spectrum of the optical counterpart of 2E 2206.6+4517 observed on 1998 May 30. The strong Balmer emission lines are indicative of a dMe star in an active flare state.

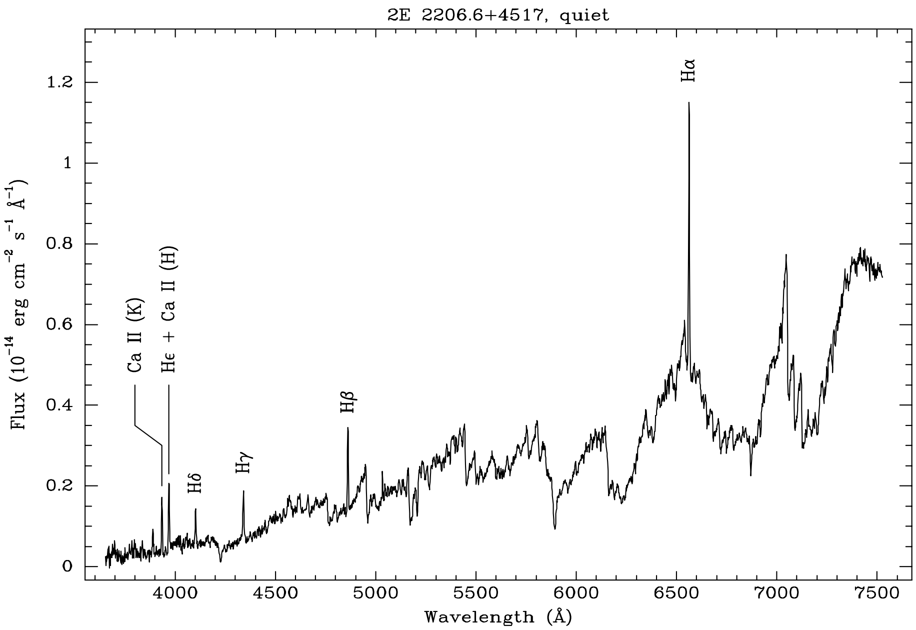

Figure 3. A second optical spectrum of 2E 2206.6+4517 was obtained on 1998 June 24. The decrease in the emission line strengths, as compared with the spectrum obtained one month earlier, could be attributed to a decrease or lack of flare activity.

Table 2. Optical emission line equivalent widths.

Date ID	1998 May 30 EW (Å)	1998 June 24 EW (Å)
H11[a] λ3771	6.7	–
H10[a] λ3798	13.6	–
H9 λ3835	23.0	7.6
H8+He I λ3889	26.6	9.2
Ca II(K) λ3934	24.1	22.7
Hε+Ca II(H) λ3970	48.6	19.6
Hδ λ4102	33.8	9.4
Hγ λ4340	43.4	10.6
He I λ4471	2.3	–
Hβ λ4861	26.2	8.4
He I[a] λ5876	1.4	–
Hα λ6563	13.0	8.0

[a] Continuum difficult to define.

emission lines of the star. To derive an accurate spectral classification, we first removed the emission lines from the spectra by interpolating to the adjacent 'continuum'. We then cross-correlated the resulting spectrum (using the IRAF FXCORR task) with a sample of digital spectra of M dwarfs from the Gliese catalogue (Henry, Kirkpatrick & Simons 1994). By far the best correlation, and a very close match was with the M3.0V star Gliese 251 (cross-correlation peak height 0.99).

For an M3.0V star, we find $M_V = 11.7 \pm 0.6$ from equation (1) of Henry et al. (1994; note that this error is the empirical rms value, more representative of the actual error than 1σ). Bessell (1991) tabulates $V - R = 1.1$ and $B - V = 1.55$ for an M3.0V star. From this we derive $M_R = 10.6$ for comparison to the USNO red magnitude, to obtain a distance of 52 pc.

4 *ROSAT* X-RAY OBSERVATIONS

4.1 Flare activity–light curve

The PSPC light curve (Fig. 4) shows prominent X-ray flare activity on 1990 June 19. Using the parameters for the best-fitting spectral model (Section 4.3), the peak flare luminosity is $L_X = 1.1 \times 10^{30}$ erg s^{-1}, a 24-fold increase over the mean quiescent luminosity $L_X = 4.6 \times 10^{28}$ erg s^{-1} (Section 4.2). The outburst can be characterized by an e-folding rise time $\tau_r \simeq 2.2$ h and decay time $\tau_d \simeq 7$ h. The total rise and decay time for the flare is $\Delta t_{rise} \simeq 6$ h and $\Delta t_{decay} \simeq 30$ h as measured from the quiescent to peak count rate. The tail end of the flare significantly departs from the exponential decay of the flare (Fig. 4).

This flare is evidently a long-duration event. Most long-decay flares on dMe stars have $\tau_d \sim 1$ h (Pallavicini et al. 1990). Recently, long-duration flares have been detected on EV Lac ($\tau_d = 10.5$ h; Schmitt 1994) and AD Leo ($\tau_d = 2.2$ h; Favata et al. 2000b). Continual heating of the flaring region during the decay has been proposed to explain such long-decaying events. Because of the long decay time, the total energy $E_{tot} = 3.5 \times 10^{34}$ erg (Table 3) released is similar to the flare seen on EV Lac ($E_{tot} = 9 \times 10^{33}$ erg; Schmitt 1994) and large compared with other dMe flare stars ($\approx 3 \times 10^{30}$–1×10^{34}; Pallavicini et al. 1990). These long-decay flares on dMe stars are, however, 2–3 orders of magnitude less energetic than giant X-ray flares on RS CVn stars such as Algol ($\tau_d = 8.4$ h; $E_{tot} = 7 \times 10^{36}$ erg; Ottmann & Schmitt 1996), and CF Tucanae ($\tau_d = 22$ h; $E_{tot} = 1.4 \times 10^{37}$ erg; Kürster & Schmitt 1996).

On 1990 July 04 at 21:11:35 UT, a flare with a peak luminosity, about the same magnitude as the PSPC out-burst (Fig. 5), was detected with the HRI. Since the HRI has extremely limited spectral resolution, we input the model fit to the PSPC flare and the HRI count rate into the IRAF/PROS task HXFLUX to convert counts to luminosity. The peak flare luminosity was $L_X = 2.9 \times 10^{30}$ erg s^{-1} a factor of 54 larger than the mean quiescent luminosity $L_X = 5.4 \times 10^{28}$ erg s^{-1}. The outburst can be characterized by an e-folding rise time $\tau_r \simeq 15$ min and decay time $\tau_d \simeq 1.2$ h. The total rise and decay time for the flare is $\Delta t_{rise} \simeq 40$ min and $\Delta t_{decay} \simeq 4.6$ h. The total energy released during the flare is $E_{tot} = 1.6 \times 10^{34}$ erg (Table 3).

We also discovered the tail end of an additional flare observed

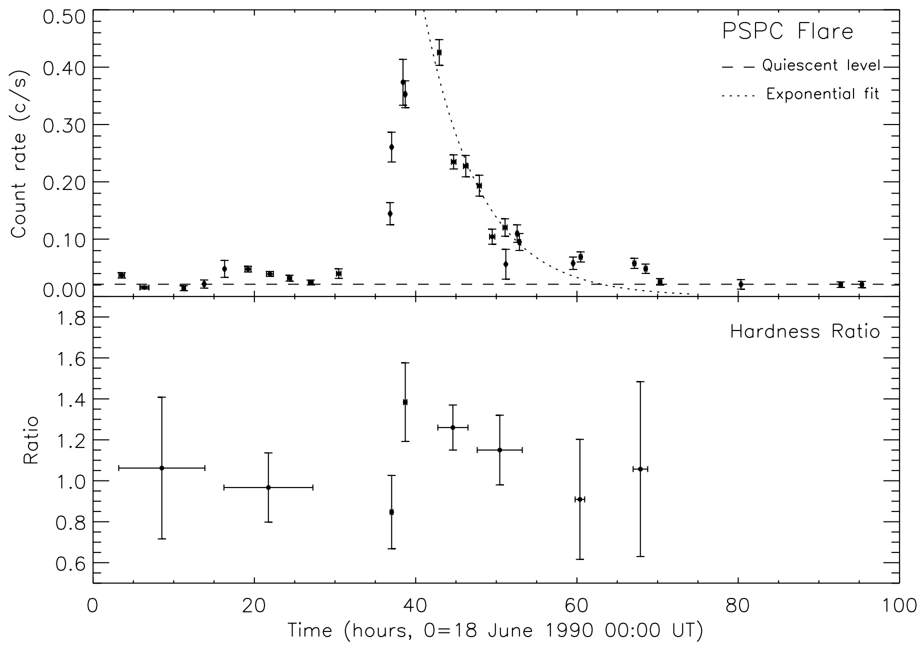

Figure 4. X-ray flare of 2E 2206.6+4517 observed with the PSPC. The flare begins on 1990 June 19 at 12:45:22 UT and lasts for 1–1.5 d. The error bars are $\pm 1\sigma$ based on count statistics. The x error bars show the time-spanned for each measurement. The broken curve is an exponential function characterized by the e-folding time, $\tau_d \simeq 7$ h. The soft and hard bands for the hardness ratio are defined as 0.07–0.42 and 0.42–2.48 keV.

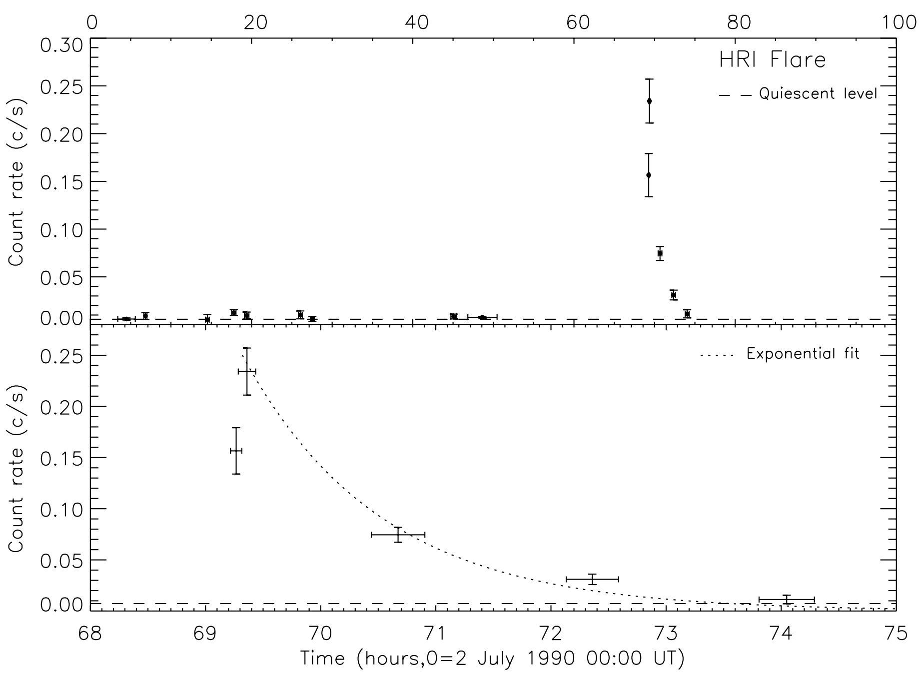

Figure 5. X-ray flare of 2E 2206.6+4517 observed with the HRI on 1990 July 4. The flare was first detected at 21:11:35 UT and lasted for 4.6 h. The lower plot focuses at the outburst in detail. The broken curve is an exponential function characterized by the e-folding time of the decay $\tau_d \simeq 1.2$ h.

Table 3. X-ray flare characteristics.

Instrument	Date	Peak (UT)	Δt_{rise}	τ_r	Δt_{decay}	τ_d	L_X (peak)	E_{tot}
PSPC	1990 June 19	12:45:22	$\simeq$6 h	$\simeq$2.2 h	$\simeq$30 h	$\simeq$7 h	1.1×10^{30} erg s^{-1}	$\simeq 3.5\times10^{34}$ erg
HRI	1990 July 4	21:11:35	$\simeq$40 min	$\simeq$15 min	$\simeq$4.6 h	$\simeq$ 1.2 h	2.9×10^{30} erg s^{-1}	$\simeq 1.6\times10^{34}$ erg
HRI	1996 June 3	–	–	–	~9 h	–	–	–

on 1996 June 03 with a two-fold rise above the background level. Because of our incomplete light curve, we can only provide an approximation to the decay time (~9 h). The X-ray characteristics of these flares are listed in Table 3.

4.2 Count rate distribution analysis: quiescent level and flaring fraction

The 'quiescent' X-ray emission outside the large flares is clearly itself variable. Fig. 4 shows a factor of 3 change in the level outside of flares, and three long HRI observations between 1995 December and 1996 July show average of $L_X = 15.4$, 6.6 and $5.0 \times 10^{28}\,\mathrm{erg\,s^{-1}}$.

To investigate this further, we performed a statistical analysis of the complete X-ray light curve to determine the minimum fraction of counts caused by flares, and the minimum fraction of time spent in a flaring state. We assumed a truly non-variable, quiescent background rate exists that can be described by a Poisson distribution. We then determined the fraction of counts caused by flares by integrating the counts left unexplained by a least-squares fit of a Poisson function to the low end of the count rate distribution (Saar & Bookbinder 1998). We averaged the results of fits using several reasonable count rate binning sizes. This analysis yields the *minimum* fraction of flare counts, since flares below the instrument sensitivity, and possible quiescent level changes owing to rotation and evolution of magnetic regions are all included in the derived quiescent level. We find that (at least) 68 ± 2 per cent of the PSPC counts and 59 ± 2 per cent of the HRI counts are caused by flares. Upper limits to the quiescent flux level and the fraction of time that the star is quiescent are also derived from the analysis. We find that the (Poisson) mean quiescent count level is $0.022 \pm 0.001\,\mathrm{count\,s^{-1}}$ for the PSPC ($L_X \approx 4.6 \pm 0.2 \times 10^{28}\,\mathrm{erg\,s^{-1}}$) and $0.0056 \pm 0.0006\,\mathrm{count\,s^{-1}}$ for the HRI ($L_X \approx 5.4 \pm 0.6 \times 10^{28}\,\mathrm{erg\,s^{-1}}$). The minimum fraction of time with a detectable flare contribution to the observed flux is 47 ± 5 per cent (PSPC) and 41 ± 8 per cent (HRI).

All of the PSPC data were taken between 1990 and 1993, while the HRI data include a significant fraction from 1995 and 1996, with an exposure-time-weighted time difference of ~1200 d. Thus it is possible that the small (~15 per cent) difference in the PSPC and HRI quiescent fluxes may be explained by time evolution of the quiet emission, owing to, for example, long-term evolution in the numbers of active regions. Unfortunately, there are relatively few quiescent counts in the 1995–96 HRI data, making a direct test of time variation inconclusive. Further data over a longer time-scale would help decide the level of the quiescent coronal variability of the star.

We find that the quiescent and bolometric luminosity agree with the linear correlation between these quantities, as noted by previous studies of flare stars (Pallavicini et al. 1990; Agrawal, Rao & Sreekantan 1986). We estimate a bolometric luminosity of $6.74 \times 10^{31}\,\mathrm{erg\,s^{-1}}$, using $M_V = 11.7$ and the bolometric correction of Pettersen (1983).

4.3 Spectral analysis

We extracted spectra from the brightest quiescent and flare PSPC images. During the longest pointing of this field, the source 2E 2206.6+4517 was in quiescence (rp100588) and 16.5 arcmin off-axis. The data set corresponding to a flare event with the highest number of source counts was rp110591, for which the source was nearly on-axis (4.4 arcmin).

For the quiescent X-ray emission, we found that no single-component thermal plasma (Raymond & Smith 1978) model could adequately fit the data. Unfortunately, the signal-to-noise ratio of our spectrum was not sufficient to uniquely constrain a two-component model. However, we found that models that did not contain a Raymond–Smith component of $kT \approx 1.0$ keV could be rejected (i.e. $\chi^2_\nu \gg 1$). These models significantly underpredict emission from approximately 0.85–1.0 keV, corresponding to the Fe L-shell blend. However, with an appropriate 'high'-temperature thermal plasma model, the remaining low-temperature emission has χ^2_ν statistics of much less than one, indicating that the models are not well constrained. Despite the poorly constrained two-component model, the spectral fit suggests the existence of a coronal plasma of $kT \approx 1$ keV. A comparison of the normalizations of the two models shows that the 'hot' and 'cool' components contribute nearly equal flux in the PSPC band (Table 4).

Because of the fewer counts in the flare observation, a larger binning factor was necessary to provide a significant signal-to-noise ratio for spectral fitting. However, we could not fit the resulting spectrum with any one- or two-component model. The heavy binning broadens the effect of uncertain calibration features, particularly the PSPC window carbon edge at 0.4 keV. To compare the quiescent and flare spectra, we must mitigate this effect. The peaks and troughs in the spectra most affected by binning all occur below about 1 keV. Using only the photons above 1 keV has the added advantage that the 'hot' component dominates in this regime, so we may use a single-temperature model. We fit both spectra in the energy range 1.0–1.8 keV with a single-temperature Raymond–Smith model, using the value of N_H from the full quiescent spectrum.

A direct comparison of the flare and quiescent normalization shows an increase by nearly a factor of 20 in the emission measure. In addition, though the temperatures are not very well constrained, their 1σ errors just barely overlap, indicating that the increase in X-ray emission was likely to be accompanied by an increase in the plasma temperature. This is consistent with behaviour seen during flares in late-type active stars (e.g. Giampapa et al. 1996; Singh et al. 1999).

The small number of counts does not allow a determination of a temperature variation during the flare decay. To investigate the spectral evolution of the flare, we calculated hardness ratios (Fig. 4). The count distribution appears to harden by about 40–50 per cent during the onset of the flare. A decrease of the hardness ratio during the decay is evident without certainty owing to limited count statistics.

Table 4. X-ray spectral model fits.

	Model	N_H (cm^{-2})	kT (1) (keV)	Norm (1)	kT (2) (keV)	Norm (2)	χ^2_ν
Quiescence	RS+RS	5.0×10^{19}	0.16[a]	4.8×10^{-5}	0.97[a]	6.8×10^{-5}	0.66
Quiescence	RS	5.0×10^{19}	$0.99^{+0.3}_{-0.2}$	6.8×10^{-5}	–	–	0.33
Flare	RS	5.0×10^{19}	$1.32^{+0.7}_{-0.3}$	1.3×10^{-3}	–	–	0.66

[a] The one-sigma error is not bounded.

Singh et al. (1999) found that Fe abundances for active dwarf stars with $\log(L_X/L_{bol}) > -3.7$ are strongly subsolar, whereas the Fe abundances in the less active stars are within a factor of 2 of the solar value. Since the quiescent luminosity ratio for 2E 2206.6+4517 hovers near this value, low abundances may also affect our X-ray spectral fits. On the other hand, flare activity has been observed to increase the apparent elemental abundances (Ottman & Schmitt 1996).

5 CONCLUSION

In this paper, we have identified a new flare star 2E 2206.6+4517 using extensive *ROSAT* X-ray observations and optical spectra. The object has been classified as a M3.0Ve star. Three large X-ray flare events are seen with light curves characteristic of outbursts detected in other flare stars. Two flares with almost complete X-ray coverage show a variation in strength and time-scales. A flare detected with the PSPC had a peak luminosity $L_X = 1.1 \times 10^{30}\,\mathrm{erg\,s^{-1}}$, an e-folding rise time of $\approx$2.2 h and a decay time of $\approx$7 h. We interpret this long-decay time (one of the longest ever observed) as possible evidence for continual heating as similar to recent observations and analysis of AD Leo and EV Lac (Favata et al. 2000a; Schmitt 1994). An observation with the HRI detected a flare with a higher peak luminosity of $L_X = 2.9 \times 10^{30}\,\mathrm{erg\,s^{-1}}$, an e-folding rise time of $\approx$15 min, and a decay time of $\approx$1.2 h.

We used a statistical analysis of the X-ray light curves to measure the quiescent X-ray level, the (minimum) fraction of counts in flares and (minimum) fraction of time that the star exhibits flare or microflare activity. The PSPC data showed a quiescent luminosity of $L_X = 4.6 \pm 0.2 \times 10^{28}\,\mathrm{erg\,s^{-1}}$, with $\geqslant 68 \pm 2$ per cent of counts coming from flares, and a significant flare contribution to at least 47 ± 5 per cent of the time observed. The HRI data, taken on average almost 3 yr later, show a quiescent luminosity of $L_X = 5.4 \pm 0.4 \times 10^{28}\,\mathrm{erg\,s^{-1}}$, with $\geqslant 59 \pm 2$ per cent of counts coming from flares, and a significant flare contribution to at least 41 ± 8 per cent of the time observed.

We obtained two optical spectra that show strong and variable emission lines of the hydrogen Balmer series and neutral helium which is further evidence for flare activity.

With the large amount of X-ray coverage of the source 2E 2206.6+4517 in the *ROSAT* data archive, this object provides an excellent opportunity to facilitate in the understanding of the physical properties of these flare stars including the flare, quiescent and long-term activity. Further measurements of this object may be afforded by calibration observations of AR Lac by *Chandra* or *XMM-Newton*.

ACKNOWLEDGMENTS

We would like to thank the reviewer, J. Schmitt, and J. Drake for their useful comments on this manuscript, and Rick Harnden and Andrea Prestwich for their advice and useful discussions. Many thanks to Perry Berlind for obtaining the optical spectra, and to Susan Tokarz for their preliminary reduction. This research has made use of data obtained through the High Energy Astrophysics Science Archive Research Center Online Service, provided by the NASA/Goddard Space Flight Center. The Digitized Sky Surveys were produced at the Space Telescope Science Institute under U.S. Government grant NAG W-2166. The images of these surveys are based on photographic data obtained using the Oschin Schmidt Telescope on Palomar Mountain and the UK Schmidt Telescope. The plates are processed into the present compressed digital form with the permission of these institutions.

REFERENCES

Agrawal P. C., Rao A. R., Sreekantan B. V., 1986, MNRAS, 219, 225
Bessell M. S., 1991, AJ, 101, 662
Fabricant D., Cheimets P., Caldwell N., Geary J., 1998, PASP, 110, 79F
Favata F., Reale F., Micela G., Sciortino S., Maggio A., Matsumoto H., 2000a, A&A, 353, 987
Favata F., Micela G., Reale F., 2000b, A&A, 354, 1021
Giampapa M. S., Rosner R., Kashyap V., Fleming T. A., Schmitt J. H. M. M., Bookbinder J. A., 1996, ApJ, 463, 707
Harris D. E. et al., 1993, The Einstein Observatory catalogue of IPC X-ray sources, 7, H
Henry T. J., Kirkpatrick J. D., Simons D. A., 1994, AJ, 108, 1437
Kürster M., Schmitt J. H. M. M., 1996, A&A, 311, 211
Monet D. G., 1998, BAAS, 193, 12003
Montes D., Saar S. H., Collier Cameron A., Unruh Y. C., 1999, MNRAS, 305, 45
Ottmann R., Schmitt J. H. M. M., 1996, A&A, 307, 813
Pallavicini R., Tagliaferri G., Stella L., 1990, A&A, 228, 403
Pettersen B. R., 1983, in Byre P. B., Rodono M., eds, Activity in Red-dwarf Stars. Reidel, Dordrecht, p. 17
Raymond J. C., Smith B. W., 1977, ApJS, 35, 419
Reale F., Micela G., 1998, A&A, 334, 1028
Saar S. H., Bookbinder J. A., 1998, in Donahue R. A., Bookbinder J. A., eds, The Tenth Cambridge Workshop on Cool Stars, Stellar Systems, and the Sun (ASP CD ROM). Astron. Soc. Pac., San Francisco, p. 1560
Singh K. P., Drake S. A., Gotthelf E. V., White N. E., 1999, ApJ, 512, 874
Schmitt J. H. M. M., 1994, ApJ, 90, 735
Schmitt J. H. M. M., Favata F., 1999, Nat, 401, 44

This paper has been typeset from a TEX/LATEX file prepared by the author.